A Study to Assess the Effect of Asphalt Mixture on the Photocatalytic Performance: A Simulation

Wengang Zhang[1], Kui Hu[2,3]*, Sen Han[3], and Zhuangzhuang Liu[3]

[1] School of Architectural Engineering, Shandong University of Technology, Zibo 255049, China
[2] College of Civil Engineering and Architecture, Henan University of Technology, Xi'an 710064, China
[3] School of Highway, Chang'an University, Xi'an, 710064, China

ABSTRACT

This study reports the simulation of a photocatalytic system process and the photocatalytic property of self-cleaning asphalt concrete (SCAC) with four typical asphalt mixtures. A photocatalytic system was simulated based on the pollutant concentration data, which were collected on three types of city roads. Two photocatalytic indexes were proposed to evaluate the photocatalytic property of self-cleaning asphalt concrete: relative decomposition rate and degradation capacity. Four typical asphalt mixtures were prepared with SBS/TiO_2 modified bitumen: AC-13a asphalt mixture (AC-13a), AC-13b asphalt mixture (AC-13b), open-graded fraction courses (OGFC), and porous asphalt concrete (PAC). The performance of the SCAC samples was investigated using the cracking resistance, rutting resistance, and moisture susceptibility. The results show that the degradation capacity of CO is approximately 20 times more than that of HC and CO . The air voids of SCAC, which is exposed to ultraviolet rays, contribute to the photocatalytic indexes in the simulated system in this study. In addition, the SBS /TiO_2 modified bitumen does not improve the high- or low-temperature property and water stability of SCAC.

Keywords: Exhaust Pollutants, Self-cleaning Asphalt Concrete, Photocatalytic System Simulation, Photocatalytic Indexes

INTRODUCTION

The environmental sustainability of building and construction has become a key issue and drawn particular concern among the governments, researchers, policymakers, industries, and the public [1, 2]. Road transport is one of the main source of pollution in urban areas, which accounts for 39% and 15% of the total NOx and fine particulate matter (PM2.5) emissions respectively [3]. Furthermore, traffic-related air pollutants are associated with cardiovascular, respiratory diseases and lung cancer [4]. Some exhaust pollutants (HC, CO, and NO) in urban areas are considered to be very harmful and poisonous gases are primarily emitted from combustion [5, 6]. NOx is one of the six major pollutants and is listed as a criterion pollutant as a part of the ambient air quality standards required by the 1970 Clean Air Act [2]. Photocatalysts have been used as the "self-cleaning" material for decades, and they absolutely contribute

***Corresponding author**
Kui Hu
Email: mailhukui@163.com
Tel: +86 153 9720 8872
Fax: +86 153 9720 8872

Article history
Received: September 13, 2016
Received in revised form: August 06,2017
Accepted: August 15. 2017
Available online: May 22, 2018
DOI: 10.22078/jpst.2017.2241.1396

to better quality of life [7]. Titanium dioxide is considered the most efficient material currently used as a catalyst, particularly on the nanoscale [8, 9]. Titanium dioxide in nanosized (Nano-TiO_2) particles is a promising additive for self-cleaning concrete because it is actively photocatalytic and has a proper energy gap and high stability [10-12]. The use of TiO_2 combination with cementitious materials has shown a favorable synergistic effect in the reduction of pollutants [13, 14]. The self-cleaning asphalt concrete (SCAC) is a potential city pavement approach to make the city air clearer and cooler by transferring the air pollutants and ultraviolet ray [15]. However, the TiO_2 coating on the concrete reduces the macrostructure of the pavement or will be “washed away” by rain and vehicle tires. Previous studies focused on “catalytic material and catalytic performance” of NOx photocatalytic degradation but ignored the HC and CO pollutant, particularly for an asphalt mixture. In terms of testing system simulation, Dylla [16, 17] setup a simulating system with a photocatalytic testing device that provided an enclosed controlled environment. The simulated ultraviolet rays and atmosphere consist of a pollutant source, an air source, adjustable valves, a humidifier, a calibrator, a photocatalytic reactor, and an NO analyzer. Meng [18] designed and built a stainless steel simulation reactor for the indoor purification examination. Osborn [19] measured the NOx removal photocatalytic efficiency in the laboratory under controlled conditions according to a standard method of Japanese Industrial Standards. Ortelli [20] performed a comparative study to investigate the photocatalytic activity and efficiency of the modified TiO_2 nanomaterials and to identify the suitable analytical method to probe the photocatalysis in self-cleaning textiles. However, the current evaluation of SCAC was not matched with the practical conditions in urban area.

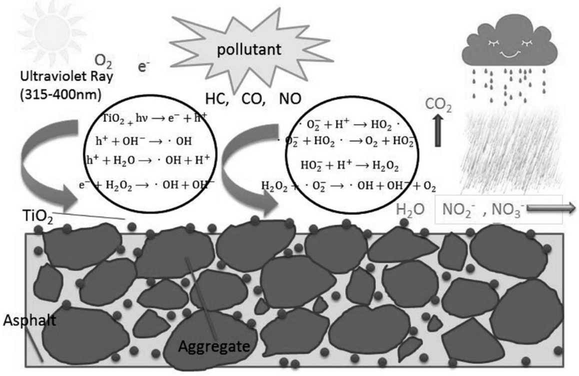

Figure 1: Photocatalytic process of asphalt mixture

In this paper, highly active TiO_2/SBS asphalt modified with nanometer titanium dioxide particles (Nano-TiO_2) was prepared as the binder to improve the asphalt mixture photocatalytic degradation efficiency. A proposed mode of the oxidation of CO, HC, and NO through hydroxyl radical and hydrogen ion intermediates in the presence of SCAC is presented in Figure 1. Based on the collected data on the city expressway, a new testing system was developed to match with the practical conditions. Four typical asphalt mixtures (AC-13a, AC-13b, OGFC, and PAC) were prepared to investigate the road performance and the effect of mixture types on the photocatalytic degradation property.

EXPERIMENTAL PROCEDURES

Photocatalytic System Simulation

Pollutant Concentration Collection

The objective of the device in Figure 2a was to measure the vehicle emissions in an urban area. Because the photocatalytic property of SCAC is affected by the CO, HC, and NO concentrations during the catalytic reaction process [21]; the testing environment must match with the practical conditions in the photocatalytic property test of SCAC. The vehicle pollutant analyzer (Figure 2a) in this study was FGA-4100(5G), which was produced by Foshan Analytical Instrument Co., Ltd. The parameters of the analyzer are listed in Table 1. The dynamic change of the HC, CO, CO_2, O_2, and NO concentration was detected and recorded in a computer. Vehicle emissions in urban area can be measured under controlled conditions in the laboratory [22]. Dynamometer facilities are designed under the regulatory standards [23]. To obtain the gas concentration on the road, three types of road conditions were selected to collect the concentrations of CO, HC, and NO. As shown in Figure 2a, the traffic conditions for the concentration collection in this study were a city expressway in rainy weather in Xi'an, China, a city expressway in sunny weather in Xi'an, China, and a tunnel in Qinling mountains, China. Figure 2b displays the collecting experiment in rainy weather on the expressway. To match with practical conditions, the gas detector was hold above the pavement surface approximately 20 cm. The data on the gas concentration of CO, HC, and NO collected on the city road are shown in Figures 3-5.

Table 1: Testing parameters of the simulation system.

Gas	Concentration range		Relative error		Sensitivity	
	value	Unit	value	Unit device volume /cm^3	value/10^{-6} Vol.	unit
HC	0-9999	ppmvol.	±5	%	1×10^{-6}	Vol.
CO	0-10	Vol.	±5	%	0.01×10^{-2}	Vol.
NO	0-5000	ppmvol.	±4	%	1×10^{-6}	Vol.
O_2	0-25	Vol.%	±5	%	0.1×10^{-2}	Vol.
CO_2	0-20	Vol.%	±5	%	0.1×10^{-2}	Vol.

(a)

(b)

Figure 2: (a) the test route in Xi'an city; (b) A schematic of emission measurement.

As shown in Figure 3, the CO concentration in rainy weather is lower than that in sunny weather. Furthermore, the CO concentration in the tunnel was 0.25-0.50%, which was much higher than that on the city expressway. The CO concentration for the three types of road is in the order of tunnel > city expressway in sunny weather > city expressway in rainy weather. Moreover, the result during 30 minutes was unstable and mainly affected by the passing vehicles.

The HC concentration distributions for the three types of road are shown in Figure 4. In the rainy weather, its value was 0-20 ppm and much lower than the HC concentration in the sunny weather and the tunnel. The HC concentration was 15-35 ppm in the tunnel. The HC concentration for the three types of road ranks in the order of tunnel > city expressway in sunny weather > city expressway in rainy weather, and the total concentration level is much lower than the CO concentration.

Figure 5 displays the NO concentrations collected on the three types of road. The NO concentration is in the order of tunnel > city expressway in sunny weather > city expressway in rainy weather, which also shows that the total concentration level is even lower than the HC concentration. The concentration in rainy weather remained the lowest, while NO was concentrated in the tunnel. In general, the concentrations of CO, HC, and NO in the three types of road are in the order of tunnel > city expressway in sunny weather > city expressway in rainy weather. CO, HC, and NO were diluted in the moisture environment and concentrated in the tunnel. Meanwhile, ultraviolet ray was an essential factor for the photocatalytic process of SCAC [11, 12]. Therefore, the pollutant concentrations collected on the city expressway in sunny weather were selected as the practical situation. The maximum concentrations of CO, HC, and NO taken into consideration are 20, 45, and 18 ppm respectively.

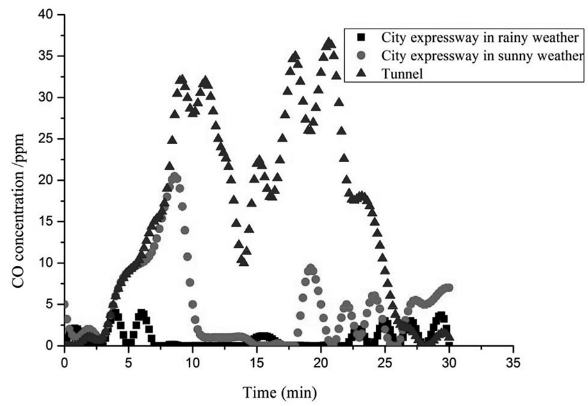

Figure 3: CO concentration data collection.

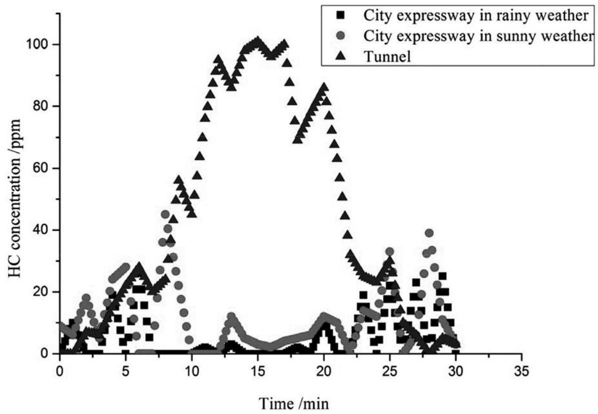

Figure 4: HC concentration data collection.

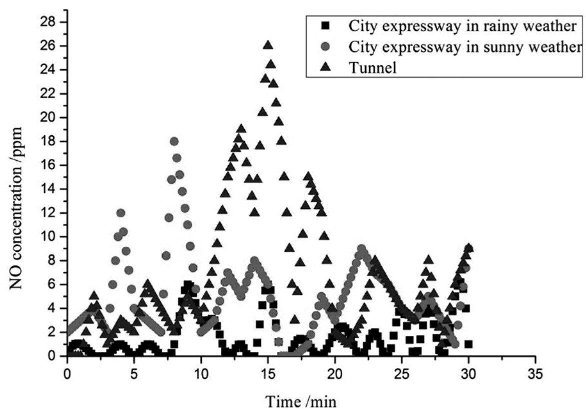

Figure 5: NO concentration data collection.

Photocatalytic System Simulation

The photocatalytic system was designed to simulate the photocatalytic property of asphalt mixtures as shown in Figure 6. The photocatalytic reactivity of SCAC was simulated by using CO, HC, and NO as the target pollutants. In Table 2, the source of gas was mixed by CO, HC, and NO at the concentration and proportion collected on the city expressway in sunny weather and was multiplied by ten. Then, the mixed gas was compressed and stored in a cylinder (produced by Xi'an Saide Instrument & Equipment Co., Ltd.) as shown in Figure 6b. The CO, HC, and NO concentrations can be detected and analyzed by a vehicle pollutant analyzer as shown in Figure 6b. Figure 6a displays the photocatalytic system designed in this study, which consists of three parts: a gas concentration analyzer (part A), a reactor device (part B), and a supply device (part C). When testing, the mixed gas flows from part C to part B. The photocatalytic reactivity of SCAC proceeds in the reactor device (part B), and the concentrations of CO, HC, and NO were detected in the gas concentration analyzer (part A). The details of the testing system simulation, composed of three parts, are described as follows.

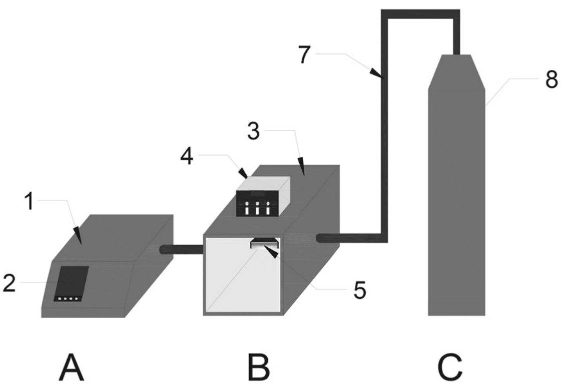

(a)

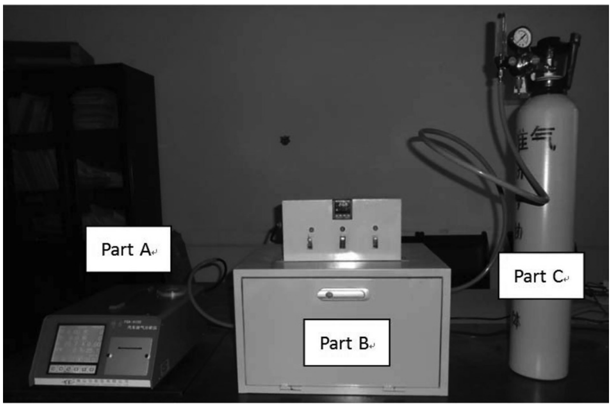

(b)

Figure 6: Photocatalytic testing system units; 1: gas analyzer; 2: gas concentration display; 3: reactor device; 4: controller; 5: electricity heating tube; 7: pipeline; 8: vehicle exhaust container.

Part A: The sensors installed in part A are NO, HC, NO, CO_2, O_2, and pressure sensors; the sensors collect the gas concentration data from part B. Six sensor data points are displayed on a digital screen. The CO_2, O_2, and pressure sensors were installed to verify the testing results. The sensors may be corroded if they are placed in the lab for too long, so a correction experiment should be performed to verify the accuracy of the air concentration results. A tube that links part A and B should be tightly sealed in the testing period.

Part B: The reactor device includes a temperature controller, a light source, a light source controller, a blender, an electricity heating tube, and a reaction cell. The reaction cell was tightly sealed during the testing period after part C turned off the gas transport. The asphalt mixture slab was placed at the bottom of the reaction cell to simulate the working condition of the pavement.

Part C: The supply device stores the testing gas as a compressed air. The gas can be pure or a mixture collected from the exhaust of vehicles or prepared from the laboratory. The gas flow speed was controlled by a valve. The gas concentration and other parameters in the supply device are shown in

Table 1, based on the data collected on the city road.

Table 2: Testing environment provided by the simulation system.

Gas	Gas Flow Speed	Gas Flow Times	Gas Input Volume	Reactor Device Volume	Concentration	Error Range
	$cm^3.s^{-1}$	s	cm^3	cm^3	ppm	ppm
CO	1.667	16	26.667	45790	200	±30
HC	1.667	16	26.667	45790	450	±10
NO	1.667	16	26.667	45790	180	±15

Raw Materials

Titanium dioxide nanocomposites (anatase, diameter 5-25 nm, surface area 40-60 m^2g^{-1}) were produced from Aladdin Industrial Corporation. The macro and micro morphology images (Figure 7) were captured using a camera and scanning electron microscope (SEM) respectively. The SBS modified asphalt with a penetration of 69 (0.1 mm at 25°C, 100 g, and 5 s), a ductility of 262.0 (mm at 5°C), and a softening point of 78.1°C (SK Asphalt Company Co., Ltd.) was used in this study. All the samples were made from basalt aggregate (2.67 g/cm^3). The titanium dioxide nanocomposites were thoroughly mixed with the SBS modified in the container at 175°C for an hour. The qualified aggregate (basalt) with a density of 2.87 g/cm^3 and mineral filler with a density of 2.81 g/cm^3 were used in this study.

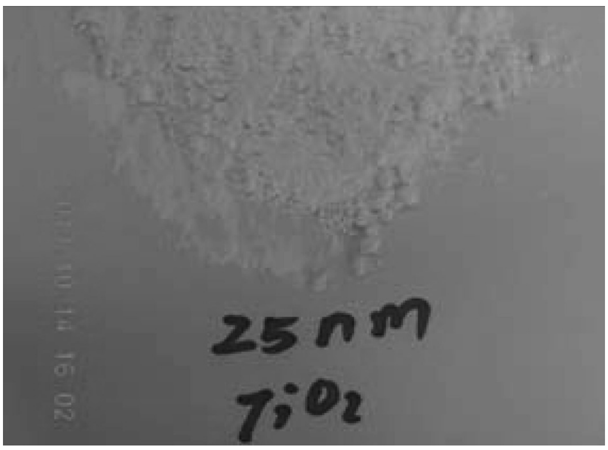

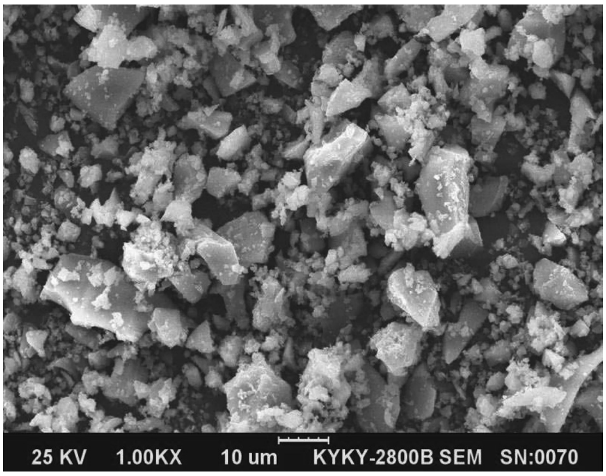

Figure 7: Morphology of titanium dioxide nanocomposites.

Preparation of Mixtures

In the experiments, the aggregates and SBS-modified asphalt were preheated at 180 °C and 170 °C in the oven respectively. Then, the liquid asphalt was mixed with the aggregate in a mixing machine. After 90 s, the mineral powder was added and mixed for 60 s. Afterwards, the hot mixture was placed in the steel frames and compacted at 145 °C to obtain the specimens, namely a Marshall specimen (101.6 mm×63.5 mm), a block (300 mm×300 mm×50 mm), and a prismatic (250 mm×30 mm×35 mm), according to the standard JTG E20-2011 (standard test method of bitumen and bituminous mixtures for highway engineering), which is the national standard of China. The prismatic specimen was compacted three times, and the AC-13 mixtures were compacted four times for comparison. Then, the rutting test (T 0719-2011), freeze-thaw splitting test (T 0729-2000), and bending test (T 0715-2011) were carried out in this study.

Four types of mixtures were used herein: AC-13 (compacted six times), AC-13 (compacted twenty-four times), OGFC-13, and PAC (described as A, B, C, and D) In the controlled mixture, SBS-modified bitumen without nano-TiO_2 was used as the binder, and the AC-13 mixture was compacted twenty-four times. The gradation, asphalt content (AC), and air voids of the asphalt mixtures are shown in Table 2.

Photocatalytic Test

Table 3 shows the relative decomposition rate ($dr_{t\cdot CO/HC/NO\cdot T}$) and the absolute decomposition rate ($\eta_{t\cdot CO/NO/HC\cdot T}$) of nano-$TiO_2$ on different types of asphalt mixture graduations such as AC-13 (compacted 3 times), AC-13 (compacted 4 times), OGFC-13, and PAC. The nano-TiO_2 content in the asphalt mixture is 2.5 wt.%, and the average particle size is 0.3 µm. The size of the asphalt mixture samples was 300 mm×300 mm×70 mm, and the tests were conducted at 25 °C and at an ultraviolet intensity of 26.64W/m^2. In this study, the experiment was divided into three stages to simulate the pavement conditions. The asphalt mixture samples (300 mm×300 mm×50 mm) were prepared and placed in a constant-temperature oven for at least five hours. After the temperature of the test system became constant, the testing gas (vehicle exhaust gas etc.) was flowed at a speed of 1.667 cm^3/s for more than 18 seconds. The gas analyzer device was turned on and set the timer to zero when the inside gas concentration became stable (CO= 200 ppm, HC+ 450 ppm, NO= 180 ppm). The gas concentrations were recorded every five minutes after the gas analyzer was turned on for 6 seconds. The entire test was competed when the timer reached 60 minutes.

Photocatalytic Indexes

To evaluate such a system, the accuracy of the test was determined using the gas sensor in the reactor device (Figure 6 part B). Gas sensors have different operating parameters such as the gas range, error margin, and distinguishing precision, which should be considered in the experiment as operating parameters for this system.

The photocatalytic degradation process used to evaluate the test system was divided into three stages in this study. At the first stage, the photocatalytic reactions proceeded at a fast rate compared to the slight growth in the second stage. The nano-TiO_2 with a high reactivity had more molecular reaction opportunities at the beginning. The chemical reaction slowed down, until the reaction reached a thermodynamic equilibrium. At the third stage, the relative decomposition percentage declined instead of increasing as expected properly because of the inhibition of the photocatalytic activity of nano-TiO_2.

Table 3: Mixture laboratory results.

Mixture	Sieve size (mm)										AC (wt.%)	Air Voids (%)
	16.00	13.20	9.50	4.75	2.36	1.18	0.60	0.30	0.15	0.075		
A	100.00	96.75	83.27	44.07	35.21	24.03	19.20	12.69	9.40	5.69	4.8	10.2
B	100.00	96.75	83.27	44.07	35.21	24.03	19.20	12.69	9.40	5.69	4.8	4.1
C	100.00	93.08	64.74	14.27	11.49	9.01	7.98	6.49	5.37	3.70	5.0	18.2
D	100.00	92.40	43.50	11.20	9.10	7.50	6.90	6.0	5.6	5.0	5.0	21.3
Control	100.00	96.75	83.27	44.07	35.21	24.03	19.20	12.69	9.40	5.69	4.8	4.1

Photocatalytic Test

Table 3 shows the relative decomposition rate ($dr_{t\cdot CO/HC/NO\cdot T}$) and the absolute decomposition rate ($\eta_{t\cdot CO/NO/HC\cdot T}$) of nano-$TiO_2$ on different types of asphalt mixture graduations such as AC-13 (compacted 3 times), AC-13 (compacted 4 times), OGFC-13, and PAC. The nano-TiO_2 content in the asphalt mixture is 2.5 wt.%, and the average particle size is 0.3 µm. The size of the asphalt mixture samples was 300 mm×300 mm×70 mm, and the tests were conducted at 25 °C and at an ultraviolet intensity of 26.64W/m^2. In this study, the experiment was divided into three stages to simulate the pavement conditions. The asphalt mixture samples (300 mm×300 mm×50 mm) were prepared and placed in a constant-temperature oven for at least five hours. After the temperature of the test system became constant, the testing gas (vehicle exhaust gas etc.) was flowed at a speed of 1.667 cm^3/s for more than 18 seconds. The gas analyzer device was turned on and set the timer to zero when the inside gas concentration became stable (CO= 200 ppm, HC+ 450 ppm, NO= 180 ppm). The gas concentrations were recorded every five minutes after the gas analyzer was turned on for 6 seconds. The entire test was competed when the timer reached 60 minutes.

Photocatalytic Indexes

To evaluate such a system, the accuracy of the test was determined using the gas sensor in the reactor device (Figure 6 part B). Gas sensors have different operating parameters such as the gas range, error margin, and distinguishing precision, which should be considered in the experiment as operating parameters for this system.

The photocatalytic degradation process used to evaluate the test system was divided into three stages in this study. At the first stage, the photocatalytic reactions proceeded at a fast rate compared to the slight growth in the second stage. The nano-TiO_2 with a high reactivity had more molecular reaction opportunities at the beginning. The chemical reaction slowed down, until the reaction reached a thermodynamic equilibrium. At the third stage, the relative decomposition percentage declined instead of increasing as expected properly because of the inhibition of the photocatalytic activity of nano-TiO_2.

Nano-TiO_2 photocatalytic degradation is a notably attractive method to remove CO, HC, and NO from the vehicle exhaust because it enables the transformation of pollutants into harmless gaseous compounds such as CO_2, H_2O, and NOx in the outdoor environment. Two indexes were put forward to evaluate the photocatalytic property of asphalt mixture based on the catalytic property of nano-TiO_2: the relative decomposition rate and the absolute decomposition rate.

The relative decomposition rate ($dr_{t\cdot CO/HC/NO\cdot T}$) is defined as the degradation rate between the reductions of gas concentration in time period of 0-*t* and the gas concentration of the standard specimen at time *t*. The relative decomposition percentages of CO, HC, and NO were calculated using Equations 1 to 3:

$$dr_{t.CO.T} = \frac{C_{t.CO.T} - C^{c}_{t.CO.T}}{C_{t.CO.T}} \times 100 \quad (1)$$

$$dr_{t.HC.T} = \frac{C_{t.HC.T} - C^{c}_{t.HC.T}}{C_{t.HC.T}} \times 100 \quad (2)$$

$$dr_{t.NO.T} = \frac{C_{t.NO.T} - C^{c}_{t.NO.T}}{C_{t.NO.T}} \times 100 \quad (3)$$

where, $dr_{t\cdot CO\cdot T}$, $dr_{t\cdot NO\cdot T}$,and $dr_{t\cdot HC\cdot T}$ are the relative decomposition rates of CO, HC, and NO respectively. $C^c_{t\cdot CO\cdot T}$, $C^c_{t\cdot NO\cdot T}$, and $C^c_{t\cdot HC\cdot T}$ are the gas concentrations of the testing samples at moment *t*; $C_{t\cdot CO\cdot T}$, $C_{t\cdot NO\cdot T}$, and $C_{t\cdot HC\cdot T}$ are the gas concentrations of the standard samples at moment *t*, and *T* is the testing temperature.

The absolute decomposition rate ($\eta_{t\cdot CO/NO/HC\cdot T}$) is defined as the weight of the decomposed gas. The sample area for each sample is used in this evaluation index. The absolute decompositions of CO, HC, and NO were calculated using Equations 4 to 6:

$$\eta_{t\cdot CO\cdot T}= m_{t\cdot CO\cdot T}/m_c= (C_{t\cdot CO\cdot T}- C^c_{t\cdot CO\cdot T})\times 45790\ cm^3\times\rho_{CO}/m_c \quad (4)$$

$$\eta_{t\cdot HC\cdot T}= m_{t\cdot HC\cdot T}/m_c= (C_{t\cdot HC\cdot T}- C^c_{t\cdot HC\cdot T}) \times 45790cm^3 \times \rho_{HC}/m_c \quad (5)$$

$$\eta_{t\cdot NO\cdot T}= m_{t\cdot NO\cdot T}/m_c= (C_{t\cdot NO\cdot T}- C^c_{t\cdot NO\cdot T}) \times 45790cm^3 \times \rho_{NO}/m_c \quad (6)$$

Where, $\eta_{t\cdot CO\cdot T}$, $\eta_{t\cdot NO\cdot T}$, and $\eta_{t\cdot HC\cdot T}$ are the absolute decomposition rates of CO, HC, and NO respectively; m_c is the nano-TiO_2 content.

The absolute decomposition rate is evaluating the whole degradation ability of asphalt mixture. On the other hand, the relative composition rate of CO, HC, and NO is evaluating the degradation ability of TiO_2 distributed in the asphalt.

RESULTS AND DISCUSSION

Engineering Performance

To investigate the engineering performance of SCAC, the rutting test (Figure 8), freeze-thaw splitting test (Figure 9), and bending test (Figure 10) were performed. The rutting test result largely depends upon the mixture types instead of the nano-TiO_2 mix in the binder, as indicated in Figure 8. Sample B and the control samples with lower air voids had higher dynamic stabilities (DS) of 8574 cycle/mm and 8360 cycle/mm respectively. Sample C and D with high air voids of 4.1% had lower DS property than sample B and the control sample. The lowest rutting test result (3240 cycle/mm) appeared in sample A since sample A was compacted six times, which was only a quarter of the dynamic stability of normal samples. The permanent deformation performance is significantly affected by the type of asphalt modifier[24]. The gradation type, the degree of compaction, air voids, nominal maximum aggregate size, and asphalt type are the main factors for the high-temperature performance of asphalt mixtures [25]. In the comparison between mixture B and the control sample, the nano-TiO_2 additives showed no significant effect on the rutting test result.

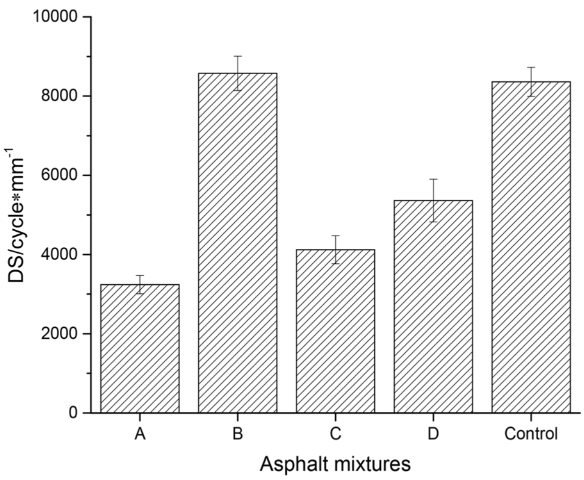

Figure 8: Rutting test.

Figure 9 shows the low-temperature property of SCAC using the bending test method. Sample A had the highest flexural strain value of 4230 because of the degree of compaction. An increase in air void ratio results in a decrease in low-temperature performance. The asphalt mixture B showed a lower flexural strain than the control sample. Meanwhile, the air voids ratios of asphalt mixture significantly affect the low-temperature performance, as indicated in samples B, C, and D.

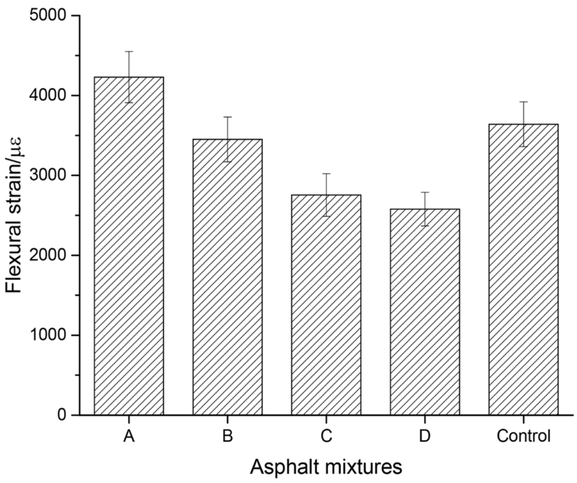

Figure 9: Low-temperature bending test.

Figure 10 shows the susceptibility to moisture damage using the freeze-thaw cycle test. The results indicate that the TSR index is related to the air void ratio. The mixture with a lower air void ratio (4.1% for both sample B and control sample) had a higher TSR value. The additive nano-TiO_2 reduced the TSR value compared to the mixture B and control sample. Possible reasons contributing to this phenomenon are as follows: (1) the nano-TiO_2 component in the binder reduces the adhesive ability between SBS-modified asphalt and aggregate. The SBS polymer strengthens the asphalt because of the similar organic material properties. Meanwhile, the incompatibility of inorganic (mineral) nano-TiO_2 and SBS-modified asphalt decreases the adhesion property; (2) the nano-TiO_2 particles are easily dissolved in water and remove a certain amount of binder during the freeze-thaw cycle test. In addition, mixture A with a compaction degree of six times had a TSR value of 72%, which was 16% lower than the normal compaction degree of twenty-four times.

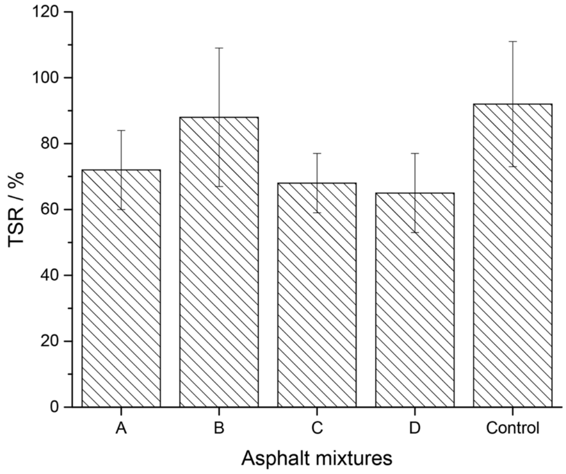

Figure 10: Freeze-thaw cycle test.

The engineering performance of SCAC was mainly determined by the gradation type, degree of compaction, and air voids instead of the addition of nano-TiO_2 in the SBS-modified asphalt. Furthermore, the asphalt mixtures with nano-TiO_2 additives in the binder were less susceptible to moisture damage possibly because TiO_2 is more soluble in water than in asphalt, particularly in a nanosized form.

Relative Decomposition Rate

As shown in Figure 11, the relative decomposition rates ($dr_{t\cdot CO/HC/NO\cdot T}$ of SCAC were relatively high and stable for all the types of mixtures except the control sample without TiO_2 additive. The photocatalytic nanosized TiO_2 material proved to be a good additive for exhaust pollutants (CO, HC, and NO) with high relative decomposition rates of over 20%.

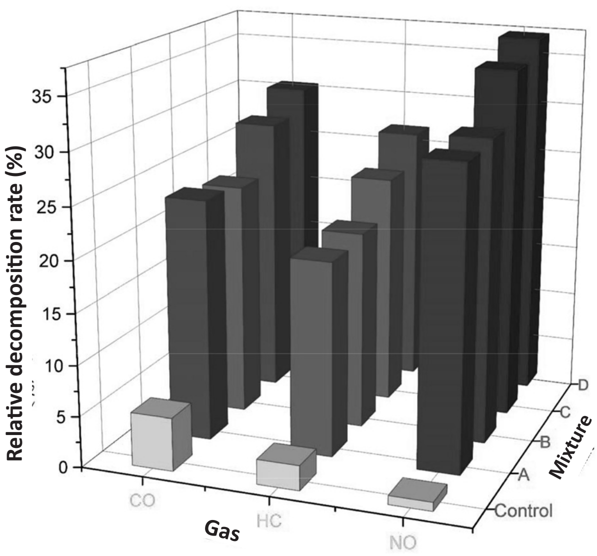

Figure 11: Relative decomposition rates of CO.

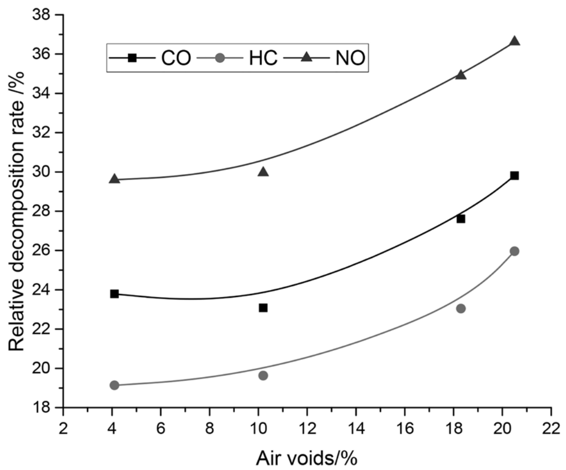

Figure 12: Relative decomposition rate and air voids.

The CO, HC, and NO photocatalytic reactions for SCAC and the control mixture were in the order of D > C > A > B > control sample. A similar trend of relative decomposition rate was obtained in terms of the air voids of SCAC, as shown in Figure 12. When the air voids increased from 4.10 to 21.30%, the relative decomposition of CO increased from 23.79 to 29.81. Meanwhile, the relative decomposition rates of HC and NO increased from 19.14 to 25.96% and to 29.60% respectively. The result indicates that the photocatalytic property is determined by the effective contact area of ultraviolet rays and TiO_2 particles. During the self-cleaning process, the amount of TiO_2 particles exposed to the ultraviolet ray dominates the photocatalytic reactions on the surface of SCAC.

For the TiO_2 particles exposed to the voids without ultraviolet ray, the photocatalytic reaction can hardly occur because of the lack of sunlight. Thus, the ultraviolet ray is the essential factor for photocatalytic reaction instead of the air voids, which is consistent with the reports of Janusz Lasek [21].

Degradation Capacity

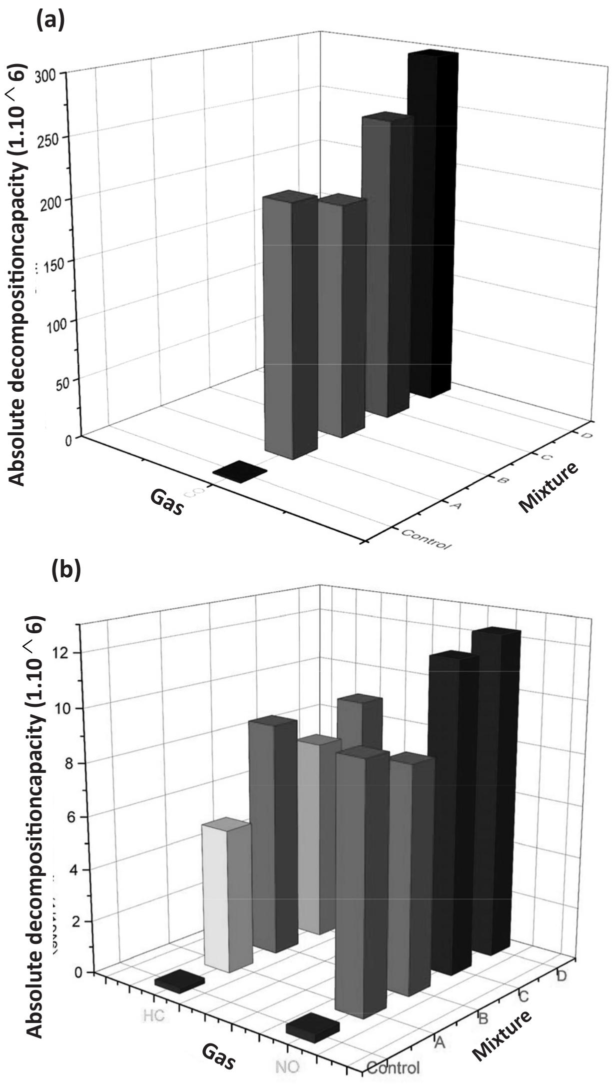

Figure 13: Degradation capacity of (a) CO (a) and (b) HC and NO.

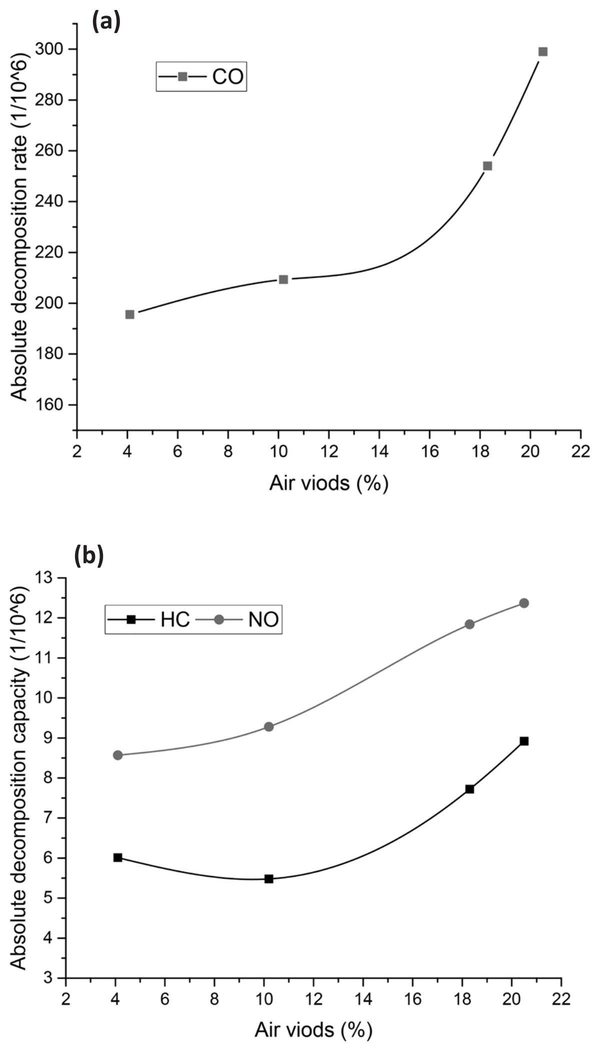

Figure 14: Degradation capacity and air voids of (a) CO and (b) HC and NO.

The degradation capacity of CO, HC, and NO is shown in Figure 13. TiO_2 generates photocatalytic reactions, as shown in the control mixture and SCAC samples. The degradation capacity of CO was in the order of D > C > A > B > the control sample. Meanwhile, the degradation capacity of HC and NO were respectively in the order of D > B > C > A > the control sample and in the order of D > C > A > B > the control sample. The TiO_2 photocatalytic ability of CO was more than twenty times higher than that of HC and NO on the index of degradation capacity. Thus, CO has a much higher photocatalytic degradation rate than the other two pollutants. Figure 14 shows the degradation capacity and air voids of SCAC. The degradation capacity slowly increased with air voids, particularly for HC and NO (Figure 14b). Hence, the photocatalytic actions rely on the proportion of TiO_2 particles exposed to the ultraviolet ray instead of the air voids of SCAC. TiO2 particles act as a catalyst and are excited by the ultraviolet ray for the reactions to occur:

$CO \rightarrow H_2CO_3 \rightarrow CO_2$,

$NO \rightarrow HNO_2 \rightarrow HNO_3$,

$HC \rightarrow H_2O + CO \rightarrow H_2O + CO_2$.

The SCAC in this study can be a self-cleaning agent for CO, HC, and NO pollutants under ultraviolet ray. Therefore, to enhance the photocatalytic property, using SCAC with high air voids is not recommended in this study.

CONCLUSIONS

The photocatalytic concrete was widely studied but because of the characteristic of city roads, no simulation system matched the actual pollutant concentrations before this paper. A new evaluating system and testing equipment were simulated based on the pollutant data collected on the city expressway in sunny weather. Since the pollutants of CO, HC, and NO were diluted by the moisture of the environment and concentrated in the tunnel, the pollutants concentration in the sunny weather was selected as the database to simulate the photocatalytic test system. Two indexes were proposed to evaluate the photocatalytic degradation property of SCAC: relative decomposition rate and degradation capacity. The photocatalytic reactions of CO, HC, and NO were performed and compared for AC-13 (compacted six times), AC-13 (compacted twenty-four times), OGFC-13, and PAC with air voids of 10.2, 4.1, 18.2, and 21.3%. The results revealed that the self-cleaning asphalt concrete with nanosized TiO_2 powder had superior photocatalytic degradation activity for HC and NO, and particularly for CO pollutants.

The increase in photocatalytic efficiency is consistent with the air voids at a slow rate. Photocatalytic actions rely on the proportion of TiO_2 particles exposed to ultraviolet rays instead of the air voids of SCAC. Thus, this study does not recommend enhancing the photocatalytic property using high air voids SCAC.

It is well known that nano-TiO_2 can be functionalized for pollutant degradation and transfer the heating energy from sunlight. It is a promising material for asphalt pavement to make the city cleaner and cooler. However, TiO_2 additive is very expensive for city road construction when mixing with asphalt mixture, particularly in nanosized form. In addition, the TiO_2 coating on the concrete reduces the macrostructure of the pavement or will be washed away by rain and vehicle tires. An effective method for further application of TiO_2 in city road construction remains to be discussed.

ACKNOWLEDGEMENTS

The authors acknowledge the financial support for this study provisioned by: Foundation for Young Scientist in Shandong Province, China (2015BSB01264), funds of the Natural Science Foundation Committee (NSFC) of China (No. 51578076), Research Start-up Fund for Ph.D. in Shandong University of Technology (414040). The contents of this paper reflect the views and opinions of the authors, who are responsible for the accuracy of data presented herein. This study was conducted in the Key Laboratory for Special Area Highway of Ministry of Education in Chang'an University, China. As such, the authors acknowledge the support that has made this laboratory and the operations possible.

NOMENCLATURES

SCAC	: Self-cleaning Asphalt Concrete
SEM	: Scanning Electron Microscopy
AC-13a	: Asphalt Concrete-13a
AC-13b	: Asphalt Concrete-13b
OGFC	: Open-graded Fraction Courses
PAC	: Porous Asphalt Concrete

REFERENCES

1. Chiarini A., "Designing an Environmental Sustainable Supply Chain through ISO 14001 Standard. Management of Environmental Quality," *An International Journal*, **2012**, *24*(1), 16-33.
2. Tao Z., Hewings G., and Donaghy K., "An Economic Analysis of Midwestern US Criteria Pollutant Emissions Trends from 1970 to 2000. Ecological Economics," **2010**, *69*(8), 1666-1674.
3. Caserini S., "Impact of the Dropping Activity with Vehicle Age on Air Pollutant Emissions," *Atmospheric Pollution Research*, **2013**, *4*(3), 282-289.
4. Hoek G., "Long-term Air Pollution Exposure and Cardio-respiratory Mortality: A Review," *Environmental Health*, **2013**, 12.
5. Ishihara, H., "Paper-structured Catalyst for Catalytic NOx Removal from Combustion Exhaust Gas," *Chemical Engineering Science*, **2010**, *65*(1), 208-213.
6. Klingenberg H. and Winneke H., "Studies on Health Effects of Automotive Exhaust Emissions

How Dangerous are Diesel Emissions?," *Science of the Total Environment*, **1990**, *93*, 95-105.

7. Cassar L., "Photocatalysis of Cementitious Materials," in International RILEM Symposium on Photocatalysis, Environment and Construction Materials, **2007**.
8. Sun B., Smirniotis P. G., and Boolchand P., "Visible Light Photocatalysis with Platinized Rutile TiO_2 for Aqueous Organic Oxidation," *Langmuir*, **2005**, *21*(24), 11397-11403.
9. Mitsionis A., "Hydroxyapatite/titanium dioxide nanocomposites for controlled photocatalytic NO oxidation," *Applied Catalysis B-Environmental*, **2011,** *106*(3-4), 398-404.
10. Ghafar H. H., "Preparation of Carbon Coated FeWO 4 and its Photocatalytic Activity under Visible Light," *Open Materials Science Journal*, **2008**, *2*, 56-59.
11. Portela R. and Hernández-Alonso M. D., "Environmental Applications of Photocatalysis, in Design of Advanced Photocatalytic Materials for Energy and Environmental Applications," *Springer*, **2013**, 35-66.
12. Paz Y., "Application of TiO_2 Photocatalysis for Air Treatment: Patents' Overview," *Applied Catalysis B: Environmental*, **2010**, *99*(3), 448-460.
13. Cassar L., "Photocatalysis of Cementitious Materials: Clean Buildings and Clean Air," *Mrs Bulletin*, **2004,** *29*(05), 328-331.
14. Trapalis A., "TiO_2/graphene Composite Photocatalysts for NOx Removal: A Comparison of Surfactant-stabilized Graphene and Reduced Graphene Oxide," *Applied Catalysis B-Environmental*, **2016**, *180*, 637-647.
15. Shen W., "Preparation of Titanium Dioxide Nano Particle Modified Photocatalytic Self-cleaning Concrete," *Journal of Cleaner Production*, **2015**, *87*, 762-765.
16. Dylla H., "Laboratory Investigation of the Effect of Mixed Nitrogen Dioxide and Nitrogen Oxide Gases on Titanium Dioxide Photocatalytic Efficiency in Concrete Pavements," *Journal of Materials in Civil Engineering*, **2010**, *23*(7), 1087-1093.
17. Dylla H., Hassan M., and Osborn D., "Field Evaluation of Ability of Photocatalytic Concrete Pavements to Remove Nitrogen Oxides, Transportation Research Record," *Journal of the Transportation Research Board*, **2012,** 2290, 154-160.
18. Chen M. and Chu J. W., "NO x Photocatalytic Degradation on Active Concrete Road Surface from Experiment to Real-scale Application," *Journal of Cleaner Production*, **2011,** *19*(11), 1266-1272.
19. Osborn D. J., "Quantification of NOX Reduction via Nitrate Accumulation on a TiO_2 Photocatalytic Concrete Pavement," Faculty of the Louisiana State University and Agricultural and Mechanical College MSc, Louisiana State University, **2012**.
20. Ortelli S., "Multiple Approach to Test Nano TiO_2 Photo-activity," *Journal of Photochemistry and Photobiology a-Chemistry*, **2014**, *292*, 26-33.
21. Lasek J., Yu Y. H., and Wu J. C., "Removal of NO x by Photocatalytic Processes," *Journal of Photochemistry and Photobiology C: Photochemistry Reviews*, **2013**, *14*, 29-52.
22. Franco V., "Road Vehicle Emission Factors Development: A Review," *Atmospheric Environment*, **2013,** *70*, 84-97.
23. Gao Y. and Checkel M. D., "Emission Factors Analysis for Multiple Vehicles Using an On-

board, In-use Emissions Measurement System," SAE Technical Paper, **2007**.

24. Tayfur S., Ozen H., and Aksoy A., "Investigation of Rutting Performance of Asphalt Mixtures Containing Polymer Modifiers," *Construction and Building Materials*, **2007,** *21(*2), 328-337.
25. Wang Y. and Li W., "Study on High Temperature Performance of Asphalt Mixture Based on Rutting Test," in Applied Mechanics and Materials, **2015**.